MULTIFUNCTIONAL COMPOSITES FOR THERMAL ENERGY MANAGEMENT

V. Prakash*, M. F. P. Bifano, P. B. Kaul
Department of Mechanical and Aerospace Engineering, Case Western Reserve University, Cleveland, OH 44106-7222, USA
* Corresponding author (**vikas.prakash@case.edu**)

Keywords*: multifunctional composites, thermal energy management, vertically aligned carbon nanotube composites, CNT graphitization, thermal conductivity in epoxy, tin capping layers.*

1 Introduction

When two nominally flat and smooth solid surfaces are joined together to form a dry joint, roughness on both surfaces limit the actual area of contact between the two solids to a small percentage (about 1% to 2 %) of the apparent contact area [1]. The heat flux through such an interface (neglecting radiation between the surfaces) flows by two different heat conduction paths: firstly, solid-to-solid conduction through contact points; secondly, conduction through the air trapped between non-contacting spaces. In order to decrease the thermal contact impedance and consequently increase the heat transfer rate, the air gaps formed by the mating surfaces must be replaced by a material with a higher thermal conductivity - these materials are commonly called TIMs.

The through-thickness thermal conductivity of adhesive joints currently in use is $k_z \sim 0.3$ W/m K. Based on current requirements of the aerospace industry, a through-thickness thermal conductivity of ~ 7–10 W/mK is expected to enable increased multi-functionality and lean manufacturing of systems in numerous applications such as the thermal management of both electronics and aerospace structures, and the improved energy conversion efficiency of directed energy devices.

In the present paper, the use of vertically aligned (VA) multi-walled carbon nanotubes (MWCNTs) to enhance the through-thickness thermal conductivity in the adhesively bonded joints is evaluated. TIMs that employ carbon allotropes which include CNTs, graphite, diamond, and amorphous carbon are especially attractive for increasing thermal conductivity [2-5]. Moreover, a small volume fraction of VA-CNTs is expected to enhance thermal conductivity in the through-thickness direction (perpendicular to the bond line) [3] while maintaining high mechanical integrity of the adhesive joint. By placing the CNTs perpendicular to and spanning the system components, there are no CNT/epoxy interfaces encountered in the through-thickness direction; thus, the interfacial thermal resistance between the CNT and the epoxy is minimized. In other words, the CNT and epoxy are thermally in parallel, and heat transport occurs via the path of least resistance through the VA-CNTs.

Despite efforts put forward by several research groups [3, 6, 7] these carbon nanomaterial-based TIMs are still far from being commercially available. Even though theoretical predictions show that carbon nanotubes have extremely high thermal conductivity, these estimates are mainly based on CNTs with ideal atomic structures [8-10], whereas in the real application scenario defects and impurities are expected to be responsible for lowering their thermal conductivity [11-13]. Furthermore, the contact thermal resistances between CNTs and other substances, e.g., the polymer matrix in composites [14] and/or other CNTs [15], is very high and even the functionalization of CNTs is not sufficient to consistently enhance the performance of these composites [16]. Also, CNTs have a modulus of elasticity greater than most bulk materials (>1 TPa). When aligned in a vertical arrays, the excessive stiffness of the CNT TIM may result in an increase in contact impedance with the substrates above or below the aligned CNT films [17]. Another technical barrier is the high difficulty of achieving high filling ratio and dense alignment of CNTs in the CNT-based TIMs.

In our present work, an efficient TIM system is developed using VA-MWCNTs to improve the through-thickness thermal conductivity of an adhesive joint. It is assumed that the thermal

properties of the aligned MWCNTs in the epoxy matrix are similar to those of individual MWCNTs if the quality and chirality of the MWCNTs remain the same. Furthermore, we introduce a transition zone (TZ) comprising of a tin thin film at the interface between the MWCNTs and the surrounding material to minimize thermal impedance mismatch and thermal resistance due to interfacial roughness.

Figure 1 shows a schematic of our proposed VA-MWCNT/epoxy TIM system. The overall thermal impedance of the TIM is expected to be governed by the interfacial impedances between the bounding solids and the mating surfaces of the CNT-epoxy layer. These interfaces are generally neither fully conforming nor smooth and thus, lead to a significant increment of thermal contact impedance.

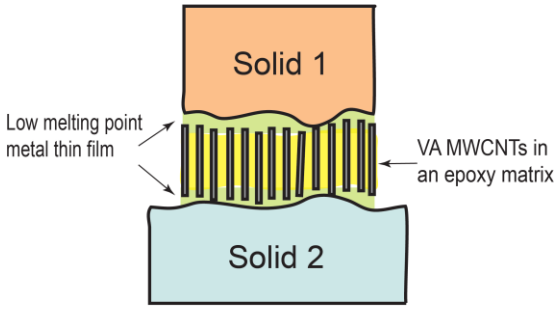

Figure 1: Schematic of VA-MWCNT TIM. The TIM facilitates heat transport between bounding solids (solid 1 and solid 2). A low melting point (Sn) thin film (green) fills the transition zones between the CNT-polymer/solid interfaces.

2 Tasks and Procedures Employed

Fabrication and characterization are performed to determine key components in improving the effective through-thickness thermal conductivity and to identify improvements in such an adhesively-jointed system. In particular we address the following:

- Synthesis and fabrication of VA-MWCNT epoxy composites.
- Characterization of thermal conductivity in individual MWCNTs as a function annealing condition (i.e. graphitized versus non-graphitized).
- Separate characterization of thermal conductivity as a function of temperature in both the epoxy matrix, and the low melting point capping layer materials, e.g., tin.
- Characterization of thermal energy transport in the VA-MWCNT composites with and without the tin capping layer.

3 Experimental Procedure and Results

The VA-MWCNT arrays used in the present investigation are procured from the laboratories of Prof Liming Dai at CWRU and Prof. Shanov at the University of Cincinnati. In Prof Dai's laboratory, VA-MWCNT arrays are grown via pyrolysis of iron (II) phthalocyanine (FePc) in Ar/H_2 at 900 ^{o}C on a silicon wafer [18, 19]. These MWCNTs are ~ 25-50 nm in diameter and have lengths varying from 2.25 mm in the middle of the turf to 2.9 mm at the edges. VA-MWCNT arrays of longer lengths (5 to 10 mm) are procured from Prof. Shanov's laboratory, which are synthesized using water-assisted chemical vapor deposition (CVD) [20-22]. The nanotube diameter of the water-assisted CVD arrays vary from 15-45 nm.

The epoxy-based carbon nanotube composites are fabricated by immersing the MWCNT array into a solution of Epon 862 epoxy comprised of EPICURE curing agent W, and acetone solvent. Prior to immersion, the epoxy is ultrasonicated using a Bransonic bath with digital heat control and timer for approximately 8 minutes. The solution is poured onto the VA-MWCNTs and spin-coated to allow the epoxy to infiltrate the array. After casting the MWCNT/epoxy composite, both surfaces are initially lapped using a Vibromat (Buehler) polisher. The surfaces are then sequentially polished with a diamond abrasive (Microid Diamond Compound) of 9, 3 and 0.5 μm while applying a 5 N constant force. Following polishing, the sample is ethanol washed and air-dried. The MWCNT tips are exposed from the epoxy by reactive ion etching (RIE) with 13.5 MHz RF plasma. Atomic force microscopy (AFM) micrographs are used to verify MWCNT tip exposure.

A capping layer of highly thermally conductivity soft metal (low yield strength) aids in the filling of surface asperities on both mating solids and thereby decreases the thermal resistance of the CNT-polymer/bounding surface interfaces (Fig 1). Moreover, the capping layer is kept relatively thin to minimize thermal resistance. In this regard, a 500 ± 50 nm layer of tin (64 W/m-K and melting point of 230 ^{0}C) is expected to be effective capping layer material.

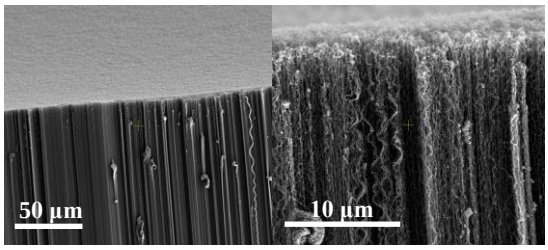

Figure 2: SEM micrographs of VA-MWCNT arrays prepared by thermal CVD.

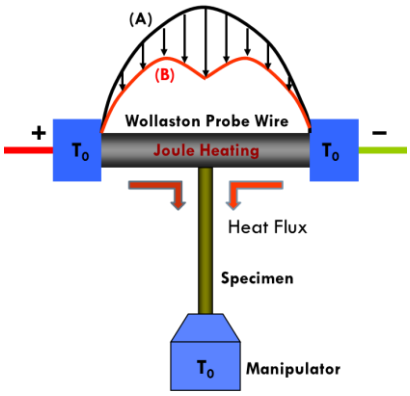

Figure 3: Schematic of the Wollaston probe wire which acts as both a heater and temperature sensor. (A) Expected temperature profile of probe wire prior to coming into contact with a specimen of unknown conductivity; (B) Expected temperature profile of probe wire following contact with specimen.

3 Thermal Transport in MWCNTs

In the present study, thermal conductivity measurements of commercially available chemical vapor deposition (CVD) grown individual multi-walled carbon nanotubes (MWCNTs) are also reported. Previous studies [23] have shown that high temperature annealing can lead to several structural and chemical improvements in MWCNTs. In particular, annealing temperatures that exceed 2250°C have been observed to produce x-ray diffraction patterns similar to those of highly graphitic MWCNTs grown by arc-discharge methods. The results also show that higher annealing temperatures up to 3000°C can promote smaller interlayer wall spacings, which is indicative of a decrease in wall defects. Residual Fe, the primary growth catalyst for MWCNTs was also found to be reduced from 7.1 % by wt. after CVD growth to less than 0.01 %. Major Fe reduction occurred both at the ends and in the core of the MWCNTs once the annealing temperature surpassed the vaporization temperature of Fe (>1800°C). It is expected that more continuous graphitic planes and a reduction of residual catalyst particles may result in an increase in phonon mean free paths, and thus lead to CNTs with higher thermal conductivity.

The thermal conductivity measurements are performed on individual free-standing MWCNTs using the three-omega-based Wollaston T-Type probe method inside a scanning electron microscope (SEM). Figure 3 depicts the Wollaston probe wire's temperature profile (a) before the specimen is placed into contact and (b) following contact with the specimen. The drop in spatially averaged temperature causes a reduction in electrical resistance and thus a measureable voltage decrease. The measured 3ω voltage across the probe wire is used to determine the thermal resistance of the specimen. Knowing the thermal resistance of the sensor allows for the thermal conductivity of the specimen to be determined [24].

Two sample groups are investigated in this study: 1) A thermal CVD MWCNT sample group, termed 'non-graphitized', composed of commercially available thermal CVD grown MWCNTs purchased from US Nanomaterials Research (US4304, US4309, US4315) and NanoLab (PD15L5-20); 2) A thermal CVD MWCNT sample group heat treated at 3000°C for 20 hours, purchased from US Nanomaterials Research (US4400, US4406, US4412). All NanoLab samples are grown at 600 ± 15 °C and all US Nanomaterials Research samples are initially grown at 665 ± 15 °C. Post growth heat-treatment of the 'graphitized' samples is performed in house by US Nanomaterials Research.

A total of 30 measurements of MWCNT conductivity are performed on both batches. 6 non-graphitized and 15 graphitized samples are measured to determine the effect of high temperature graphitization on thermal conductivity. 9 samples are omitted from the test population due to obvious gross physical deformities. 8 of the 9 rejected samples came from the graphitized sample group.

The magnitude of the thermal conductivities reported in the present study are far below the highest measured MWCNT of 3000 W/mK (Fig 12) [25]. However, the variation of specimen quality in the commercially available batches makes comparison to literature values especially difficult. The highest measured thermal conductivity is 893.0

± 170.8 W/mK for a graphitized sample having a measured OD of 35 ± 4 nm, estimated ID/OD ratio of 0.29, and length of 10.77 ± 0.04 μm. Not surprising, this sample is the straightest of all samples measured and has the least number of visible defects (Fig. 6a). The sample did not represent the majority of tested specimens and therefore was considered a statistical outlier.

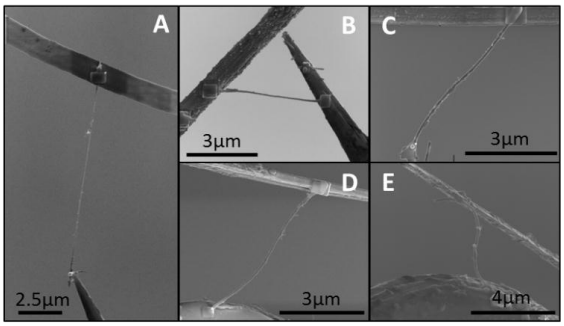

Figure 4. SEM micrographs of experiments from the graphitized sample group. In each case the Pt probe wire is pictured above the manipulator tip with sample joining the probe wire to the manipulator. (A) Sample with the highest measured thermal conductivity of 893.0 ± 170.8 W/mK, statistically considered an outlier; (B and C) Samples having the highest measured values that are within the 20% confidence interval about the graphitized group's mean, 354.6 ± 34 W/mK and 310.7 ± 48.7 W/mK, respectively; (D and E) Samples with the lowest measured values, 98.4 ±19.7 W/mK and 81.8 ± 31.1 W/mK, respectively.

The measured thermal conductivities were found to not correlate to sample length or measured outer diameter. Outer diameter measurements are expected to correlate to thermal conductivity, since smaller diameter tubes generally have fewer wall numbers permitting less inter-wall phonon scattering [26]. Following this reasoning, a single wall carbon nanotube has the highest theoretical thermal conductivity. To date, only one investigation of MWCNTs, reporting three room temperature results as a function of outer diameter has resulted in a diameter dependency [26]. However, in the present study, if a correlation between thermal conductivity and diameter of the samples tested exists, the correlation is likely to be unnoticeable due large variations in each of the sample's structural qualities.

Comparison of thermal conductivities of the non-graphitized and graphitized samples indicates that the graphitization process increases mean thermal conductivity of the graphitized group by approximately 385%.

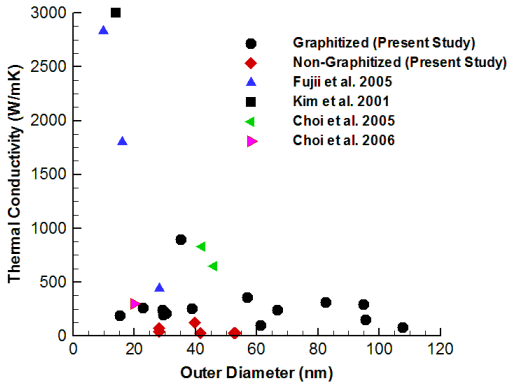

Figure 5. Thermal conductivity measurements of both graphitized and non-graphitized sample groups plotted against references [25-28].

4 Characterization of thermal conductivity in epoxy matrix, tin capping layer, and the VA-MWCNT composite TIM

The three omega technique is employed to study thermal transport in VA-MWCNT/epoxy composites as TIM materials. A complete understanding of thermal transport in composite structure must involve thermal conductivity measurements in the individual components, including the epoxy matrix, the thin tin capping layer, and the VA-MWCNT/epoxy composite. Additionally, the measurement is performed at lower temperatures to investigate the effects of increased phonon mean free paths on thermal conductivity. Another important aspect of the VA-MWCNT/epoxy composite is that it is thermally highly anisotropic. Therefore, it is essential to apply a technique that measures the thermal conductivity in directions normal (along the nanotubes) and parallel (across the nanotubes) to the composite.

Similar to the measurements performed on individual MWCNTs, the 3ω method is performed by passing a current with angular frequency ω through a heater/sensor. The heating current creates Joule heating and thus a temperature oscillation at a frequency 2ω. Subsequently, the metal heater/ sensor's electrical resistance also oscillates at 2ω, causing a measureable 3ω voltage oscillation

detected using a lock-in amplifier. The 3ω voltage oscillation is used to determine the sample's thermal properties [29, 30]. The frequency range for the experiment is chosen by examining the relationship between the film thickness, the thermal penetration depth and the heater's width. Large heater widths (as compared to sample or film thickness) produce a one-dimensional heating profile, thereby providing information about the cross-plane thermal conductivity. Narrow heater widths dissipate heat radially, and therefore with knowledge of the cross-plane thermal conductivity from the wide heater experiment, the in-plane thermal conductivity can be determined from $K^2 = K_x^2 + K_z^2$. Moreover, for an electrically conductive sample, a thin insulating film must be deposited prior to the metal line deposition to provide electrical isolation.

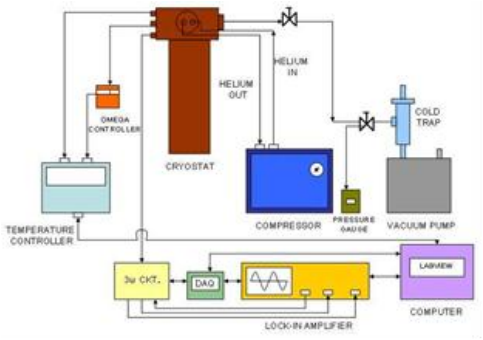

Figure 6: Schematic view of the Three Omega experimental Set-up at Case Nanomechanics Laboratory

The main components of the 3ω set-up are a cryostat (Janis Research Model: CCS-400H/204) and temperature controller that serves to regulate the sample temperature, and a lock-in amplifier to detect the voltage response of the heater (Fig. 6). The cryostat is capable of operating between the temperature range 10 K–500 K and with special thermometry can go up to 800 K. An RV-8 rotary vane pump has been used which is capable of developing a vacuum equal to 10^{-4} torr or less. The aluminum metal heater/sensor line is magnetron sputtered through a microfabricated shadow mask. The temperature coefficient of resistance of the heater/sensor is measured prior to every experiment.

The thermal conductivity of Epoxy EPON-862 is measured from 100K to 340K (Fig.7). The measured thermal conductivity of EPON-862 at room temperature is 0.224±0.02 W/m-K. The increase in thermal conductivity is expected to be the result of an increase in specific heat.

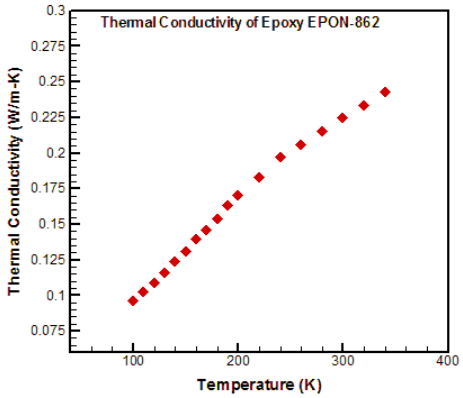

Figure 7: Thermal conductivity of epoxy resin EPON-862 with temperature.

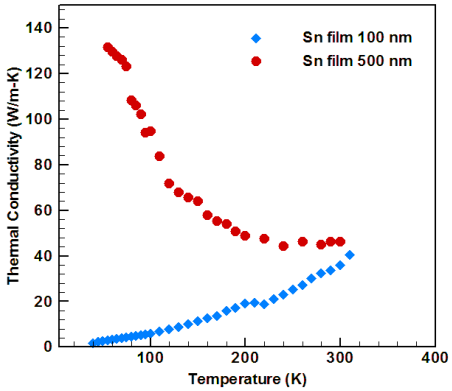

Figure 8: Thermal conductivity of a 500nm Sn film (55K-300K) and a 100nm Sn film (40K-310K)

The thermal conductivity of the 500 ± 50 nm thick film and the 100 ± 20 nm thin film show contrasting behavior with decreasing temperatures (Fig.6). The thermal conductivity of 500 nm thin film at room temperature is 46.2 ±4.2 W/m-K, which is lower when compared to its bulk value of 64 W/m-K, and increases gradually as the temperature is lowered to 55K. The thermal conductivity of the 100 nm thin film exhibits a more significant reduction in thermal conductivity (36 ± 2.88 W/m-K at 300K), when compared to bulk Sn, and decreases as the temperature is lowered. The reduction in thermal conductivity of a 100 nm Sn thin film may be due to the pronounced effects of electron

scattering at grain and twin boundaries in addition to surface boundary scattering at lower temperatures.

5 Conclusion

This research describes the systematic characterization of a model VA-MWCNT TIM system. Component level characterization that includes thermal conductivity measurements of individual MWCNTs, epoxy materials, capping layer material and thickness, as well as system level characterization of the overall VA-MWCNT/epoxy TIM with capping layers is necessary to isolate each materials contribution to the overall thermal impedance of the joint. MWCNT quality and Sn capping layer thickness is found to strongly influence each component's thermal conductivity. Because the thermal resistance of these components is in series with the bonded solids, the effective thermal conductivity of the bonded joint will undoubtedly be sensitive to each component's thermal conductivity as well as the thermal resistance at each interface. The thermal characterization of the CNT composite as a function of temperature as well as the entire TIM composite including capping layers is currently underway.

6 Acknowledgements

The authors would like to acknowledge the support of the Air Force Office of Scientific Research (AFOSR) grant FA9550-08-1-0372 and the National Science Foundation MRI grant CMMI-0922968.

7 References

1. Greenwood, J.A. and J.B.P. Williamson, Proceedings of the Royal Society of London. Series A. Mathematical and Physical Sciences, 1966. **295**(1442): p. 300-319.
2. Tong, T., et al., Ieee Transactions on Components and Packaging Technologies, 2007. **30**(1): p. 92-100.
3. Huang, H., et al., Advanced Materials, 2005. **17**(13): p. 1652-1656.
4. Yu, A., et al., The Journal of Physical Chemistry C, 2007. **111**(21): p. 7565-7569.
5. Collins, K.C. and G. Chen, ASME Conference Proceedings, 2010. **2010**(49415): p. 565-568.
6. Xu, J. and T.S. Fisher, International Journal of Heat and Mass Transfer, 2006. **49**(9-10): p. 1658-1666.
7. Yang, C., et al. *Electronic Components and Technology Conference, 2007. ECTC '07. Proceedings. 57th*. 2007.
8. Osman, M.A. and D. Srivastava, Nanotechnology, 2001. **12**(1): p. 21-24.
9. Lukes, J.R. and H.L. Zhong, Journal of Heat Transfer-Transactions of the Asme, 2007. **129**(6): p. 705-716.
10. Berber, S., Y.K. Kwon, and D. Tomanek, Physical Review Letters, 2000. **84**(20): p. 4613-4616.
11. Huang, Z., et al., Journal of Applied Physics, 2011. **109**(10): p. 104316-6.
12. Haibo, F., Z. Kai, and M.M.F. Yuen. *Electronic Materials and Packaging, 2006. EMAP 2006. International Conference on*. 2006.
13. Llaguno, M.C., et al., AIP Conference Proceedings, 2001. **591**(1): p. 384-387.
14. Shenogin, S., Journal of Applied Physics, 2004. **95**(12): p. 8136.
15. Ali, E.A. and et al., Nanotechnology, 2010. **21**(3): p. 035709.
16. Shenogin, S., et al., Applied Physics Letters, 2004. **85**(12): p. 2229-2231.
17. Cola, B.A., X. Xu, and T.S. Fisher, Applied Physics Letters, 2007. **90**(9): p. 093513.
18. Yang, Y.Y., et al., Journal of the American Chemical Society, 1999. **121**(46): p. 10832-10833.
19. Chen, W., et al., Chemical Communications, 2008: p. 163-165.
20. Hata, K., et al., Science, 2004. **306**: p. 1362-1364.
21. Shanov, V., Y.-H. Yun, and M.J. Schulz, Journal of the U. of Chem. Tech. and Metall, 2006. **41**(4): p. 377-390.
22. Yun, Y.-H., et al., Journal of Phys. Chem. B, 2006. **110**: p. 23920-23925.
23. Andrews, R., et al., Carbon, 2001. **39**(11): p. 1681-1687.
24. Dames, C., et al., Review of Scientific Instruments, 2007. **78**(10).
25. Kim, P., et al., Physical Review Letters, 2001. **87**(21).
26. Fujii, M., et al., Physical Review Letters, 2005. **95**(6): p. 065502.
27. Choi, T.Y., et al., Applied Physics Letters, 2005. **87**(1): p. 013108.
28. Choi, T.-Y., et al., Nano Letters, 2006. **6**(8): p. 1589-1593.
29. Cahill, D.G., Review of Scientific Instruments, 1990. **61**(2): p. 802-808.
30. Lee, S.M. and D.G. Cahill, Journal of Applied Physics, 1997. **81**(6): p. 2590-2595.